

## Article

# Therapeutic Effects of 30 nm Cyclosporin A-Loaded Nanoparticles Using PLGA-PEG-PLGA Triblock Copolymer for Transdermal Delivery in Mouse Models of Psoriasis

Akira Kagawa <sup>1</sup>, Akira Sato <sup>1</sup> , Kimiko Makino <sup>1</sup> and Issei Takeuchi <sup>1,2,\*</sup> <sup>1</sup> Faculty of Pharmaceutical Sciences, Tokyo University of Science, 2641, Yamazaki, Noda 278-8510, Japan<sup>2</sup> Faculty of Pharmaceutical Sciences, Josai International University, 1 Gumyo, Togane 283-8555, Japan

\* Correspondence: itakeuchi@jiu.ac.jp

**Abstract:** This study aimed to evaluate the effectiveness of poly(DL-lactide-co-glycolide)-*block*-poly(ethylene glycol)-*block*-poly(DL-lactide-co-glycolide) triblock copolymers (PLGA-PEG-PLGA) as a drug carrier in the treatment of psoriasis. Nanoparticles containing cyclosporin A (CsA) were prepared, and their cytotoxicity and skin irritation properties were investigated. These results revealed that the nanoparticles themselves had no obvious cytotoxicity or skin irritation effects. Furthermore, it was shown that loading CsA into nanoparticles promoted its cellular uptake. The therapeutic effect of CsA-loaded PLGA-PEG-PLGA nanoparticles on psoriasis was evaluated using a mouse model of psoriasis induced by imiquimod. In psoriatic skin, we confirmed that nanoparticles penetrate deep into the skin. Furthermore, it was suggested that by using PLGA-PEG-PLGA, drug carriers could reach the dermal layer, which is the target site for psoriasis treatment. The observation of skin sections after the treatment experiment showed that excessively proliferated keratinocytes were restored to an almost normal state by using PLGA-PEG-PLGA nanoparticles as drug carriers. Additionally, the quantitative measurement results for cytokines revealed that the levels of TNF- $\alpha$ , IL-17A, and IL-22 were significantly decreased compared with those of the group to which CsA suspended in a 20% ethanol solution was administered. These results indicate that PLGA-PEG-PLGA nanoparticles are promising drug carriers for the transdermal administration of CsA.

**Keywords:** transdermal delivery; cyclosporin A; nanoparticle; PLGA-PEG-PLGA; PLGA; psoriasis; mouse



**Citation:** Kagawa, A.; Sato, A.; Makino, K.; Takeuchi, I. Therapeutic Effects of 30 nm Cyclosporin A-Loaded Nanoparticles Using PLGA-PEG-PLGA Triblock Copolymer for Transdermal Delivery in Mouse Models of Psoriasis. *Appl. Sci.* **2024**, *14*, 3791. <https://doi.org/10.3390/app14093791>

Academic Editor: Gang Wei

Received: 3 April 2024

Revised: 25 April 2024

Accepted: 26 April 2024

Published: 29 April 2024



**Copyright:** © 2024 by the authors. Licensee MDPI, Basel, Switzerland. This article is an open access article distributed under the terms and conditions of the Creative Commons Attribution (CC BY) license (<https://creativecommons.org/licenses/by/4.0/>).

## 1. Introduction

Psoriasis is an inflammatory autoimmune skin disease that poses many problems including its high prevalence and chronicity, disfigurements, disability, and associated comorbidity [1]. The prevalence of psoriasis, which imposes a great psychosocial burden on patients and significantly reduces their quality of life, was reported to vary regionally and be higher in Caucasian and Scandinavian populations [1,2]. Psoriasis is classified into psoriasis vulgaris (plaque-type psoriasis), inverse psoriasis (flexural psoriasis), guttate psoriasis, and pustular psoriasis, according to its dermatological magnifications. Approximately 90% of psoriasis cases are known to correspond to chronic plaque-type psoriasis. Symptoms of psoriasis include erythema, which turns the skin red, and scales, which are raised skin and have a silvery-white scab-like appearance on the surface. It mainly affects the elbows, knees, and head, but it can spread over a wide area [3,4]. Skin cells and immune cells are involved in the pathophysiology of psoriasis. Histologically, the disease is characterized by acanthosis, which is a thickening of the epidermis, and parakeratosis, in which nuclei are retained in the stratum corneum (the outermost layer of the epidermis). In the epidermis, the granular layer is lost, and neutrophils are often accumulated in the stratum corneum. Finding parakeratosis in the stratum corneum reflects an abnormal differentiation of epidermal keratinocytes [5]. Therefore, compared with that in normal skin,

the barrier function of the stratum corneum mainly against foreign substances from the outside of the body is lowered. It was reported that psoriatic lesions are highly infiltrated by immune cells [6,7]. Pro-inflammatory cytokines produced by these cells contribute to the pathogenesis of psoriasis by causing the activation of keratinocytes and other resident skin cells [5]. Lesional T cells that secrete IL-17 (Th17 cells) were recognized as important contributors to the pathogenesis of psoriasis. Th17 cells are involved in the pathogenesis of many autoimmune and inflammatory diseases such as psoriasis, multiple sclerosis, rheumatoid arthritis, and inflammatory bowel disease [8]. Symptoms of psoriasis are caused by Th17 cells overexpressing cytokines IL-17A and IL-22. In addition, Th17 cells induced from naive T cells are maintained by IL-23 produced from dendritic cells. These IL-23-producing dendritic cells are called Tip-DCs and are major TNF- $\alpha$  producing cells [7]. Therefore, in psoriasis, TNF- $\alpha$ , IL-23, and IL-17A continuously work from the upstream to form eruptions [5]. Recently, the T helper (Th)-17/interleukin (IL)-23 axis has attracted attention in the treatment of psoriasis, as humanized anti-human IL-23p19 monoclonal antibody and humanized anti-human IL-17 monoclonal antibody, risankizumab and secukinumab were newly developed, and studies on verifying their therapeutic effects were reported [9,10]. Conventional drugs such as cyclosporin, which can be administered orally, and tacrolimus, which is used externally, are still used.

In the previous study, we successfully prepared cyclosporin A (CsA)-loaded nanoparticles with a mean diameter of 30 nm using poly(DL-lactide-*co*-glycolide)-*block*-poly(ethylene glycol)-*block*-poly(DL-lactide-*co*-glycolide) triblock copolymers (PLGA-PEG-PLGA). It was shown that PLGA-PEG-PLGA nanoparticles are better able to penetrate the skin than PLGA nanoparticles and have higher drug delivery to deep within the skin [11]. CsA is a highly lipophilic and relatively large-molecular-weight (1202 Da) drug. Its cyclic structure and large diffusional cross-section make it difficult to penetrate deep into the skin [12]. In psoriatic skin, the barrier function against external foreign substances, mainly the stratum corneum, is lowered. Therefore, we postulated that the transdermal delivery of CsA using PLGA-PEG-PLGA nanoparticles with high skin permeability would be highly effective. In this study, we investigated the effectiveness of CsA-loaded PLGA-PEG-PLGA nanoparticles with a mean volume diameter of 30 nm in treating psoriasis. The nanoparticles were prepared using PLGA-PEG-PLGA1004, a type of PLGA-PEG-PLGA, like in the previous report [11]. After evaluating the efficacy and safety of CsA-loaded PLGA-PEG-PLGA1004 nanoparticles (PLGA-PEG-PLGA1004 NPs) through cell uptake, cytotoxicity, and skin irritation tests, we conducted therapeutic experiments using psoriasis model mice. To confirm the therapeutic effect, in addition to skin morphology observation, TNF- $\alpha$ , IL-17A, and IL-22, which are important cytokines related to psoriasis, were quantified. The results of these tests were compared with those on nanoparticles prepared using poly(DL-lactide-*co*-glycolide) (PLGA NPs). PLGA NPs were prepared using the previously reported method [11].

## 2. Materials and Methods

### 2.1. Materials

PLGA (Mw: 10,000, monomer composition of DL-lactic acid/glycolic acid = 75/25) was purchased from Taki Chemical Co., Ltd. (Kakogawa, Japan). PLGA-PEG-PLGA1004 (Mw: 4000/1000/4000, monomer composition of DL-lactic acid/glycolic acid/ethylene oxide = 62/22/16) was kindly donated by Taki Chemical Co., Ltd. CsA (C<sub>62</sub>H<sub>111</sub>N<sub>11</sub>O<sub>12</sub>, purity  $\geq$  97.0%), and *N*-methyl-2-pyrrolidone (NMP, C<sub>5</sub>H<sub>9</sub>NO, purity > 98%) was purchased from Fujifilm Wako Pure Chemical Corp. (Osaka, Japan). Coumarin-6 (C<sub>20</sub>H<sub>18</sub>N<sub>2</sub>O<sub>2</sub>S, purity > 98%) was purchased from Sigma-Aldrich (St. Louis, MO, USA). DMEM (1.0 g/L glucose) with L-gln, and sodium pyruvate was purchased from Nakalai Tesque, Inc. (Kyoto, Japan). Additionally, 0.5 M EDTA (pH 8.0) and 10  $\times$  TBS Buffer (pH 7.4) were purchased from Nippon Gene Co., Ltd. (Tokyo, Japan). 3-(4,5-Dimethyl-2-thiazolyl)-2,5-diphenyl-2*H*-tetrazolium bromide (MTT, C<sub>18</sub>H<sub>16</sub>BrN<sub>5</sub>S) was purchased from Dojindo Laboratories (Mashiki, Japan). DAPI Fluoromount-G<sup>®</sup> (DAPI) was purchased from

Southern Biotechnology Associates, Inc. (Birmingham, AL, USA). 1,1-Dioctadecyl-3,3,3,3-tetramethylindotricarbocyanine iodide (DiR, C<sub>63</sub>H<sub>101</sub>IN<sub>2</sub>) was purchased from AAT Bioquest, Inc. (Pleasanton, CA, USA). Imiquimod (IMQ) cream 5% (*w/w*) was purchased from Glenmark Pharmaceuticals, Co., Ltd. (Mumbai, India). Protopic<sup>®</sup> ointment 0.1% (TAC cream, JP tacrolimus hydrate 1.02 mg/g) was purchased from Maruho Co., Ltd. (Osaka, Japan). New Hematoxylin Type M and New Eosin Type M were purchased from Muto Pure Chemicals Co., Ltd. (Tokyo, Japan). Other chemicals were of the highest reagent grade commercially available.

## 2.2. Cellular Uptake Study on PLGA-PEG-PLGA1004 NPs Using HaCaT Cells

We conducted cellular uptake tests on PLGA-PEG-PLGA1004 NPs using HaCaT cells, a human epidermal keratinocyte cell line. Epidermal thickening, one of the symptoms of psoriasis, is caused by the abnormal differentiation of epidermal cells. Immortalized HaCaT cells are widely used as model cells to mimic this condition [13]. For PLGA-PEG-PLGA1004 NPs and their comparison, PLGA NPs were prepared using a combination of an antisolvent diffusion method with preferential solvation [14,15]. An amount of 3 mL of NMP in which 4.8 mg of CsA and 75.2 mg of either polymer were dissolved was injected into 20.0 mL of purified water at a flow rate of 10 mL/s to prepare 30 nm particles [16]. To remove excess NMP and unloaded CsA, the prepared nanoparticle suspension was dialyzed for 24 h in a dialysis tube (UC36-32-100, molecular weight cut-off: 14,000, EIDIA Co., Ltd., Tokyo, Japan) [11]. Nanoparticles used in cellular uptake studies are required to contain a fluorescent substance as a tracer for observation and measurement. We prepared PLGA or PLGA-PEG-PLGA1004 NPs containing coumarin-6 by replacing CsA with coumarin-6 in the method described above [11] and conducted a cellular uptake test using HaCaT cells. We prepared PLGA or PLGA-PEG-PLGA1004 NPs containing coumarin-6, as a nanoparticle tracer, using the previously reported method [11] and conducted the cellular uptake tests using HaCaT cells. HaCaT cells were seeded on a chambered culture slide at a concentration of  $2 \times 10^5$  cells/mL and incubated for 24 h under a 5% CO<sub>2</sub> atmosphere (37 °C) to allow cells to adhere [17]. The medium was removed, and 180 µL of DMEM and 20 µL of free coumarin-6, coumarin-6-loaded PLGA NPs, or coumarin-6-loaded PLGA-PEG-PLGA1004 NPs with coumarin-6 concentration adjusted to 0.02 mg/mL were added and incubated for 2 h. After discarding the supernatant, particles adhering to the cell surface were washed with phosphate-buffered saline (PBS) and fixed with 4% (*w/v*) paraformaldehyde. Cells washed with Triton<sup>™</sup> X (0.1%) were stained and mounted with 20 µL/well DAPI and observed using a confocal laser scanning microscope (CLSM, Leica TCS SP8, Leica Microsystems, Solms, Germany) [18–20]. To evaluate the uptake of NPs by HaCaT cells, we measured the fluorescence intensity of coumarin-6 using fluorescence-activated cell sorting (FACS, BD FACSCalibur, BD Bioscience, San Jose, CA, USA). HaCaT cells were seeded in a 6-well plate at a concentration of  $5 \times 10^4$  cells/mL, and then incubated in a 5% CO<sub>2</sub> atmosphere (37 °C) for 24 h to allow the cells to adhere. The medium was removed, and 1800 µL of DMEM and 200 µL of free coumarin-6, coumarin-6-loaded PLGA NPs, or coumarin-6-loaded PLGA-PEG-PLGA1004 NPs with coumarin-6 concentration adjusted to 0.02 mg/mL were added and incubated for 2 h. Particles adhering to the cell surface were washed with PBS [20], and after deadhesion treatment was performed using a trypsin-EDTA solution, centrifugation was performed at 1300 rpm for 3 min. The supernatant was discarded, and the precipitate was redispersed in 0.5 mL of PBS. In these experiments, PBS was used as a control.

## 2.3. Cytotoxicity Test on PLGA-PEG-PLGA1004 NPs Using MTT Assay

Effects of CsA-loaded NPs on the proliferation of HaCaT cells were quantified using the MTT assay. Suppressing epidermal thickening is important in psoriasis treatment. CsA is known to increase endoplasmic reticulum stress in HaCaT cells in a dose-dependent manner, resulting in the induction of apoptosis [21]. Since this endoplasmic reticulum stress is caused by binding to cyclophilin in the cytoplasm [22], it is important to efficiently

deliver drugs into cells. HaCaT cells in the logarithmic growth phase were seeded on a chambered culture slide at a concentration of  $5 \times 10^5$  cells/mL and incubated for 24 h under a 5% CO<sub>2</sub> atmosphere (37 °C) to allow cells to adhere. The MTT assay was performed in accordance with the reagent manufacturer's protocol (Dojindo Laboratories). Free CsA, PLGA NPs, and PLGA-PEG-PLGA1004 NPs were tested at CsA concentrations of 1, 20, 50, 80, and 100 µg/mL. For comparison, similar tests were performed on blank PLGA NPs and blank PLGA-PEG-PLGA NPs, which do not contain CsA.

#### 2.4. Skin Irritation Test on PLGA-PEG-PLGA1004 NPs Using Three-Dimensional Cultured Skin

Reducing skin irritation is an important issue in formulations applied to the skin, especially in formulations containing low-molecular-weight compounds, to promote transdermal absorption [23]. The NMP used for the preparation of NPs has also been used as an absorption enhancer in transdermal administration [24]. Therefore, we investigated the skin irritation caused by PLGA-PEG-PLGA1004 NPs using LabCyte CORNEA-MODEL (Japan Tissue Engineering Co., Ltd., Gamagori, Japan), a human three-dimensional cultured corneal epithelial model. Experimental operations were performed in accordance with the attached manual. NMP containing 2.67% (*w/v*) PLGA, NMP containing 2.67% (*w/v*) PLGA-PEG-PLGA1004, 20% (*v/v*) ethanol solution (20% EtOH), PLGA NPs, and PLGA-PEG-PLGA1004 NPs were tested, and the cell viability of each was evaluated using an MTT assay. The cell viability was calculated using the following formula:

$$\text{Cell viability (\%)} = (\text{sample absorbance} - \text{blank absorbance}) / (\text{PBS absorbance} - \text{blank absorbance}) \times 100,$$

and we considered samples with cell viability below 50% to be irritating.

#### 2.5. Animal Experiments

A male BALB/cCrSlc mouse aged six weeks and a male KSN/Slc mouse aged seven weeks were purchased from Japan SLC Inc. (Tokyo, Japan). Animal care was carried out under the Guidelines for Animal Experimentation of Tokyo University of Science, which are based on the Guidelines for Animal Experimentation of the Japanese Association for Laboratory Animal Science. A mouse model of IMQ-induced psoriasis-like dermatitis (psoriasis model mouse) was produced by applying IMQ cream to the shaved dorsal skin of mice [25].

##### 2.5.1. Ex Vivo Skin Permeability Study on PLGA-PEG-PLGA1004 NPs

The transdermal delivery route of PLGA-PEG-PLGA1004 NPs was evaluated from the results of ex vivo skin permeability tests [12,16]. Skin permeability tests conducted to investigate the transdermal delivery route were performed using the psoriasis model mouse skin (psoriasis), BALB/cCrSlc mouse skin (normal skin), and KSN/Slc mouse skin (hairless skin) in the same manner as that previously reported [11]. A suspension of PLGA NPs containing coumarin-6 or PLGA-PEG-PLGA1004 NPs containing coumarin-6 that was adjusted to have a coumarin-6 concentration of 0.01 mg/mL was used as a receptor solution. As a control, a suspension in which coumarin-6 was dispersed at the same concentration in a 20% EtOH aqueous solution (coumarin-6 suspension) was used.

##### 2.5.2. In Vivo Study on the Therapeutic Effects of PLGA-PEG-PLGA1004 NPs Using the Psoriasis Model Mouse

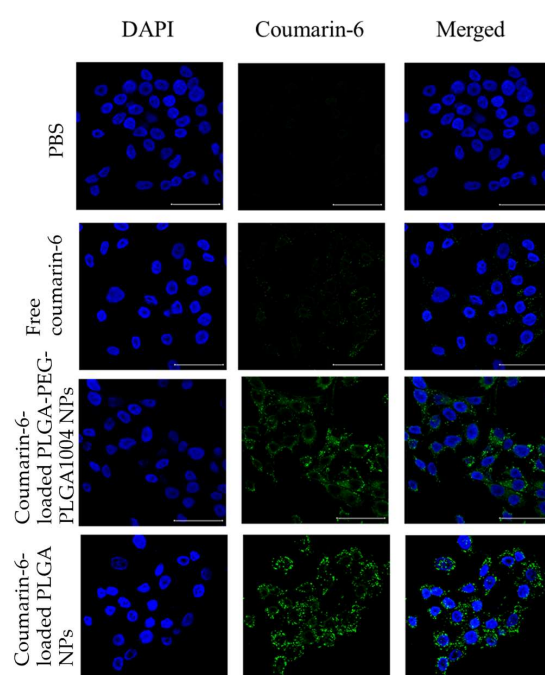
Animals were divided into six groups of five mice each: SHAM (healthy control), untreated (negative control), 20% EtOH suspension, TAC cream (positive control), PLGA NPs, and PLGA-PEG-PLGA1004 NPs. Mice in groups other than the SHAM group had 62.5 mg of IMQ cream applied to their shaved dorsal skin for 14 consecutive days starting from day 0. In the treatment group, from day 7 onwards, each sample was applied 12 h after applying the IMQ cream. To evaluate the therapeutic effects, animals were euthanized by anesthesia on day 16, and the skin and spleen were collected [26,27]. After treatment, the skin was fixed and embedded in a manner like that previously reported [11]. Skin sections

sliced to a thickness of 10  $\mu\text{m}$  using a cryostat (CM3050S, Leica Instruments, Nussloch, Germany) were stained with hematoxylin and eosin and then observed using a fluorescence microscope (BZ-9000; Keyence, Osaka, Japan). The epidermal thickness of each group was randomly selected 15–20 times and measured using ImageJ Fiji software [28–30]. Cytokine levels in the skin of each group were quantified using ELISA. The collected skin was homogenized in extract solution (10 mM Tris pH 7.4, 150 nM NaCl, 1% Triton X-100) [31], and then centrifuged to remove solids. The amounts of TNF- $\alpha$ , IL-22, and IL-17A in the obtained supernatant were quantified using LEGEND MAX™ Mouse TNF- $\alpha$  ELISA Kit, LEGEND MAX™ Mouse IL-22 ELISA Kit, and LEGEND MAX™ Mouse IL-17A ELISA Kit (BioLegend Inc., San Diego, CA, USA). We also estimated the immunosuppressive effect of CsA by calculating the spleen/body wt% from the weight of spleens removed from mice in each group after the end of the treatment experiment. The spleen is an important organ in the immune system, and the weight of the spleen is significantly involved in the immune response [32].

### 3. Results

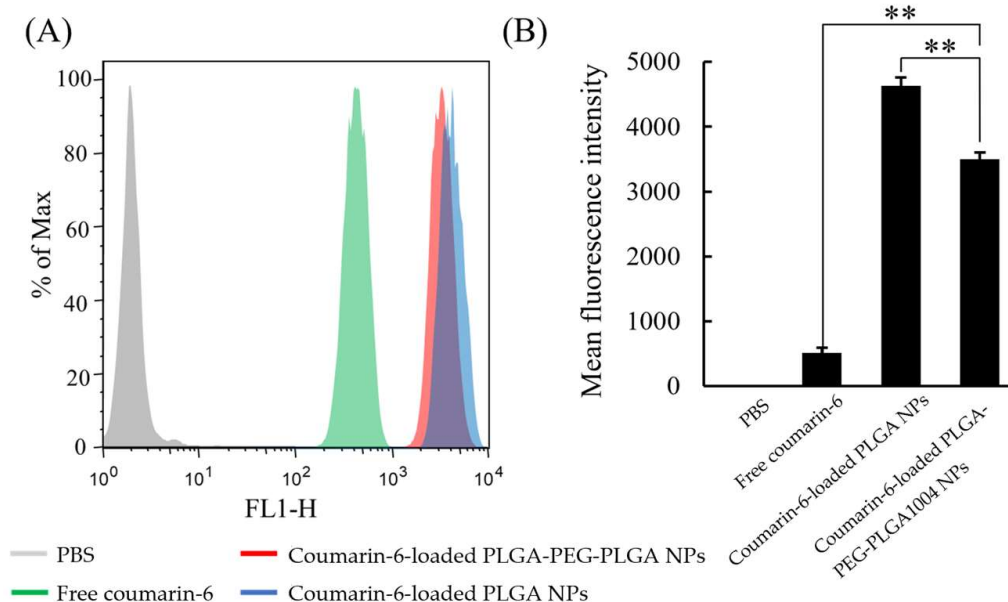
#### 3.1. Uptake of NPs by HaCaT Cells

Figure 1 shows microscopic images of the cell uptake test using the CLSM. In PBS, only the fluorescence of DAPI-stained nuclei (blue) were observed. Since NPs contain coumarin-6, they are indicated by green fluorescence derived from coumarin-6 in the figure. They showed strong fluorescence near the nucleus stained with DAPI. Therefore, it was suggested that NPs be taken into cells. Green fluorescence was also observed for free coumarin-6; however, it was much smaller than the results for the two types of NPs. Comparing the results of coumarin-6-loaded PLGA-PEG-PLGA1004 NPs and coumarin-6-loaded PLGA NPs, it was confirmed that coumarin-6-loaded PLGA-PEG-PLGA1004 NPs had weaker fluorescence intensity and lower cellular uptake. Figure 2 shows the results of measuring the fluorescence intensity of HaCaT cells using FACS. From Figure 2A,B, it was found that loading coumarin-6 into NPs facilitates its uptake into the cells, and NPs with PLGA were more easily taken up into the cells than those with PLGA-PEG-PLGA1004. These results were in good agreement with the observation results obtained using the CLSM (Figure 1).



**Figure 1.** Fluorescent images of cellular uptake tests of control (PBS), free-coumarin-6, coumarin-6-loaded PLGA-PEG-PLGA1004 NPs, and coumarin-6-loaded PLGA NPs using a confocal laser scanning

microscope. The left column, the DAPI channel, shows blue fluorescence, the middle column, the coumarin-6 channel, shows green fluorescence from the nanoparticles, and the right column represents the DAPI and coumarin-6 channels, merged (scale bar: 50  $\mu\text{m}$ ) [20].



**Figure 2.** FACS measurement results (A) and mean fluorescence intensity (B) of control (PBS), free-coumarin-6, coumarin-6-loaded PLGA-PEG-PLGA1004 NPs, and coumarin-6-loaded PLGA NPs (mean  $\pm$  S.D.,  $n = 4$ , \*\*  $p < 0.01$ , Tukey's test).

### 3.2. Cytotoxicity and Skin Irritation Due to NPs

Figure 3 shows the cell viability after 24 h measured using the MTT assay. It was confirmed that the cell viability decreased in a CsA concentration-dependent manner, and this effect was enhanced by loading CsA into NPs. As shown in Figures 1 and 2, when CsA is loaded into NPs, its uptake into cells is enhanced. In the PLGA NP administration group and the PLGA-PEG-PLGA NP administration group, it was shown that CsA was efficiently delivered into HaCaT cells and exerted its effect. Additionally, in groups to which drug-free NPs were administered, no obvious decrease in cell viability was observed, suggesting that NPs themselves have almost no cytotoxicity. The results of the skin irritation test are shown in Figure 4. In the NMP administration group, the cell viability was 27.7%. When preparing NPs, PLGA or PLGA-PEG-PLGA is dissolved in NMP and used as a good solvent [11]. Skin irritation was also confirmed in the groups administered with these good solvents (NMP + PLGA polymer and NMP + PLGA-PEG-PLGA polymer). Almost no skin irritation was observed in PLGA NPs and PLGA-PEG-PLGA1004 NPs. These results suggest that NMP in the good solvent was sufficiently removed by the NOP preparation operation.

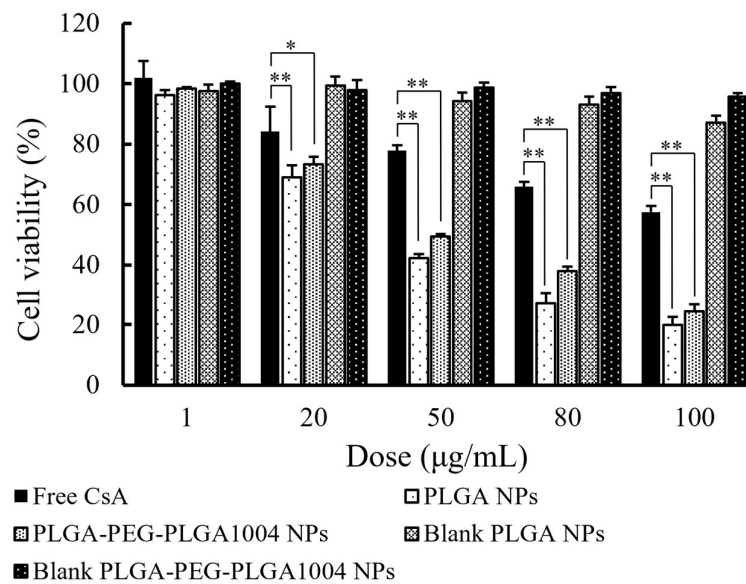


**Figure 3.** Cell viability of HaCaT cells after 24 h, measured using MTT assay (mean  $\pm$  S.D.,  $n = 4$ , \*  $p < 0.05$ , \*\*  $p < 0.01$ , Tukey's test). Blank PLGA NPs and blank PLGA-PEG-PLGA NPs refer to PLGA NPs and PLGA-PEG-PLGA NPs without CsA, respectively.

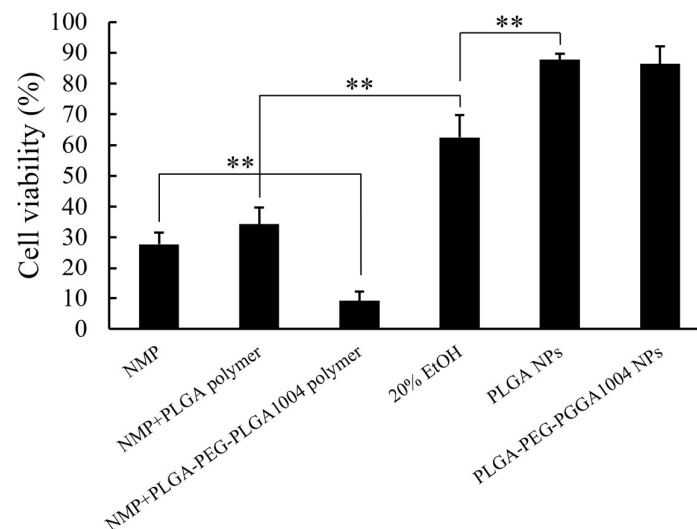


**Figure 4.** Cell viability of a human three-dimensional cultured corneal epithelial model measured using the MTT assay (mean  $\pm$  S.D.,  $n = 3$ , \*\*  $p < 0.01$ , Tukey's test).

### 3.3. Skin Permeability of PLGA-PEG-PLGA1004 NPs in Psoriatic Skin

Figure 5 shows images of skin sections observed via CLSM when coumarin-6 suspension, PLGA NPs, or PLGA-PEG-PLGA NPs were administered to psoriasis skin, normal skin, and hairless skin. We confirmed that NPs had higher skin permeability than the coumarin-6 suspension in all three types of skin. Additionally, by using PLGA-PEG-PLGA1004, NPs reached deeper parts of the skin. Coumarin-6-derived fluorescence deep in the skin was particularly strong in psoriatic skin.

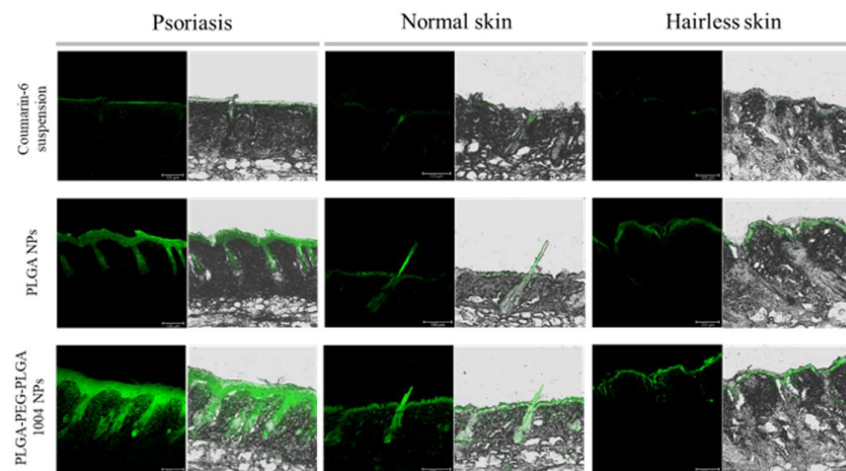


**Figure 5.** Confocal laser microscope images of cross-sections of mouse skin with the coumarin-6 suspension, PLGA NPs, and PLGA-PEG-PLGA1004 NPs at 24 h from the initiation of the ex vivo skin permeability tests (scale bar: 100  $\mu$ m). The green fluorescence comes from coumarin-6. Mouse skin was collected from the psoriasis model mouse (psoriasis skin), BALB/cCrSlc mouse (normal skin), and KSN/Slc mouse (hairless skin).

#### 3.4. Evaluation of Therapeutic Effects of PLGA-PEG-PLGA1004 NPs Using the Psoriasis Model Mouse

Images of skin sections stained with hematoxylin and eosin and numerical values of epidermal thickness for each group are shown in Figure 6A,B, respectively. Compared with that in the untreated group (“IMQ only” in Figure 6), the thickness of the epidermal layer in the treated group decreased, which confirmed that epidermal thickening was suppressed. PLGA-PEG-PLGA1004 NPs showed high therapeutic efficacy, and their efficacy was comparable to that of TAC cream (Figure 6B). Figure 7 shows images of the spleen and the spleen/body ratio ( $w/w$ ) after the end of the treatment. The increased spleen weight in the untreated group suggested that IMQ application caused an excessive production of inflammatory cytokines and immune cells. It was shown that PLGA-PEG-PLGA1004 NPs significantly suppressed the increase in spleen weight, indicating that PLGA-PEG-PLGA1004 NPs exerted a high effect on inflammatory induction.

(A)

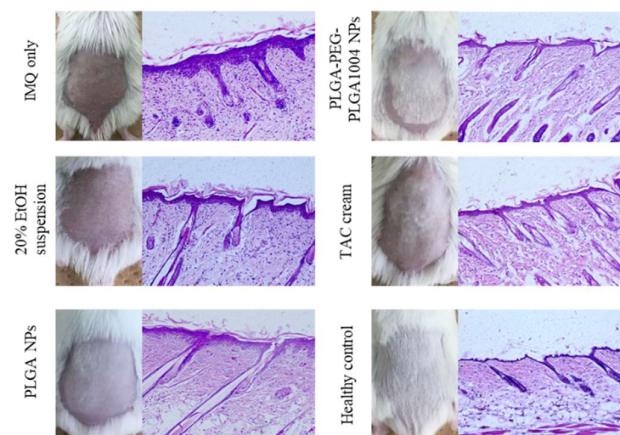


**Figure 6.** Cont.

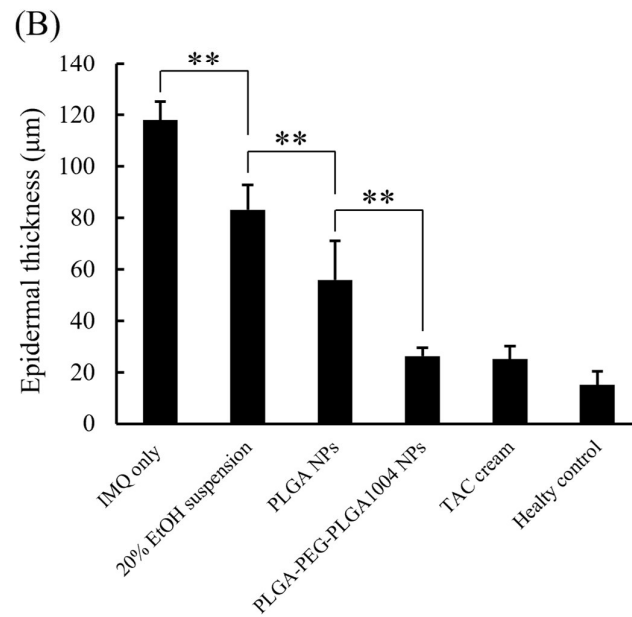


**Figure 6.** Appearance of mouse skin and images of skin sections stained with hematoxylin and eosin (A), and measurement results of epidermal thickness (B) (mean ± S.D.,  $n = 5$ ,  $** p < 0.01$ , Tukey’s test).

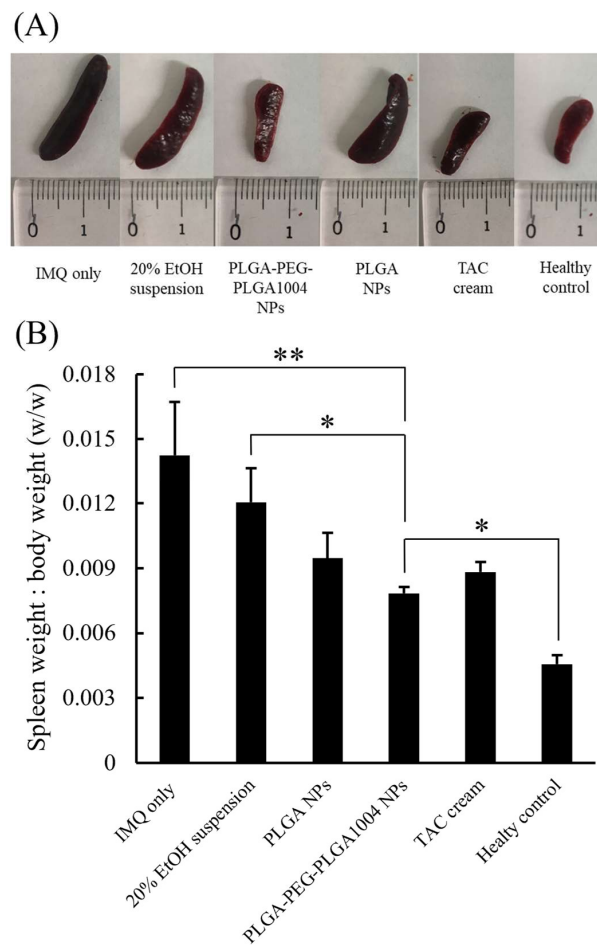


**Figure 7.** Images of spleens removed after psoriasis treatment experiments (A) and the ratio of spleen weight to mouse body weight (B) (mean ± S.D.,  $n = 5$ ,  $* p < 0.05$ ,  $** p < 0.01$ , Tukey’s test).

Figure 8 shows the produced amounts of TNF- $\alpha$ , IL-17A, and IL-22 in each group. They were increased in the untreated group, indicating that IMQ induces cytokines related to psoriasis. From the results in Figure 8, it was confirmed that PLGA-PEG-PLGA1004 NPs had a therapeutic effect equal to or greater than that of TAC cream. In the PLGA-PEG-PLGA NP administration group, all cytokine levels were significantly lower than those in the 20% EtOH suspension administration group. Moreover, those values tended to be lower than the values in other treatment groups. These indicate that the skin permeability of NPs influences the therapeutic efficacy of CsA.

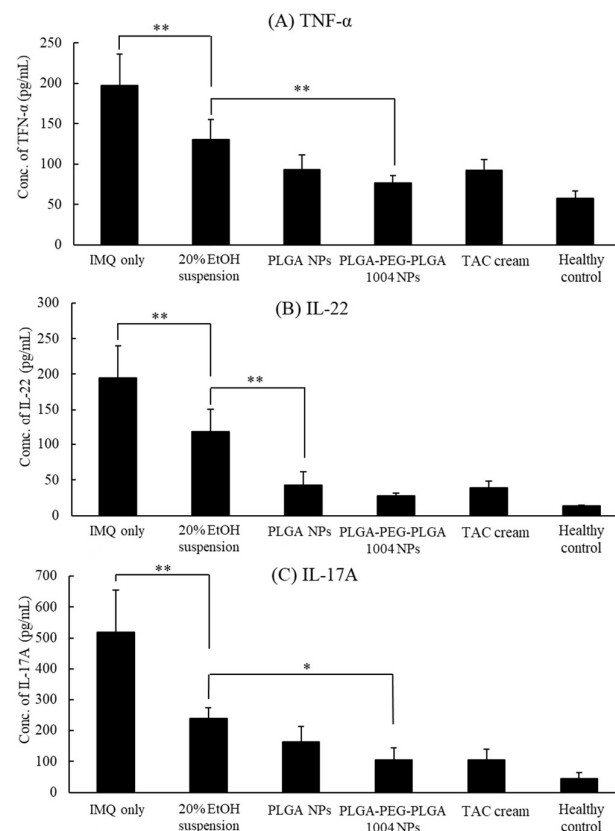


**Figure 8.** Concentrations of TNF- $\alpha$  (A), IL-22 (B), and IL-17A (C) in the skin after psoriasis treatment experiments, quantified using ELISA (mean  $\pm$  S.D.,  $n = 5$ , \*  $p < 0.05$ , \*\*  $p < 0.01$ , Tukey's test).

#### 4. Discussion

The results shown in Figures 1 and 2 confirmed that NPs are useful for the cellular uptake of hydrophobic substances. Compared with PLGA NPs, PLGA-PEG-PLGA NPs had lower cellular uptake. We considered that steric hindrance by PEG prevented the interaction of NPs with the cell membrane [33], and improved hydrophilicity, which made it difficult to be taken up into the cells [34], was responsible for the decreased cellular uptake of PLGA-PEG-PLGA1004 NPs. In the skin permeation test, as shown in Figure 5, it was found that PLGA-PEG-PLGA NPs reached deeper into the skin of psoriasis-like skin than PLGA NPs did. It is known that psoriatic skin has a faster turnover cycle than normal skin [35]. As a result, intercellular lipids are not sufficiently produced in psoriatic skin compared with normal skin, resulting in decreased barrier function and increased transepidermal water loss [36]. Due to these factors, the intercellular spaces in psoriatic skin are wider than those in normal skin, and it was reported that 40 nm FluoSpheres<sup>®</sup> were delivered deep into the skin in the psoriasis model mouse [37]. Therefore, we considered that PLGA-PEG-PLGA1004 NPs were useful for delivering CsA to the vicinity of cells rather than inside cells.

The therapeutic study using the psoriasis model mouse suggested that PLGA-PEG-PLGA1004 NPs have a high therapeutic effect on psoriasis. Th1 and Th17 are mainly involved in psoriasis, and CsA exerts its therapeutic effect by suppressing TNF- $\alpha$  (Th1), IL-17A (Th17), and IL-22 (Th17), produced by these cells. Symptoms are also caused by TNF- $\alpha$ , IL-23, IL-17A, and IL-22 in the psoriasis model mouse. TNF- $\alpha$  activates Th17 cells as well as dendritic cells and has the effect of promoting the proliferation of epidermal cells via IL-22. In addition, TNF- $\alpha$  is also produced by psoriatic lesion epidermal cells and is known to be significantly involved in the pathology of psoriasis [38]. The effects of IL-17A on epidermal cells include an increased expression of antibacterial peptides such as LL-37, the induction of inflammatory cytokine and chemokine production from epidermal cells, the promotion of neutrophil migration to the epidermis, and the proliferation of epidermal cells [39]. IL-22 is significantly involved in epidermal thickening and cooperates with Th17 to activate Stat3 and promote keratinocyte proliferation [40]. Suppressing the cytokines (IL-17A, IL-22) produced by Th17 is effective in treating psoriasis in humans as well as in the psoriasis model mouse. Therefore, the reduction in the levels of these cytokines observed in this treatment experiment may correlate with therapeutic efficacy in humans [41]. We also confirmed that hair grew due to the administration of NPs. It is also known that applying CsA to mouse skin has a hair growth effect [42,43]. These results suggest the usefulness of NPs for the treatment of psoriasis.

## 5. Conclusions

This study showed that PLGA-PEG-PLGA NPs are promising drug carriers in psoriasis treatment. Although it is difficult to directly compare them with TAC cream, which was used as a positive control, because it contains a different drug, it was suggested that PLGA-PEG-PLGA NPs have at least the same therapeutic effect as TAC cream. Research on the use of PLGA-PEG-PLGA as NPs for transdermal administration is at an early stage, and many issues need to be investigated in the future, such as the size of the NPs, their surface charge, and the composition of the polymer. The results of this study will contribute to the application of CsA to external preparations and will promote the use of PLGA-PEG-PLGA in drug delivery systems.

**Author Contributions:** Conceptualization, A.K. and I.T.; methodology, A.K. and I.T.; software, A.K. and I.T.; validation, A.K., K.M. and I.T.; formal analysis, A.K. and I.T.; investigation, A.K.; resources, A.S., K.M. and I.T.; data curation, A.K. and I.T.; writing—original draft preparation, A.K. and I.T.; writing—review and editing, A.S. and I.T.; visualization, A.K. and I.T.; supervision, K.M. and I.T.; project administration, K.M. and I.T.; funding acquisition, K.M. and I.T. All authors have read and agreed to the published version of the manuscript.

**Funding:** This work was supported by JSPS KAKENHI Grant Numbers JP18K14888 and JP22K06553.

**Institutional Review Board Statement:** The animal study protocol was approved by the Ethics Committee of Tokyo University of Science (protocol code: Y18044 (April 2018) and Y19042 (April 2019)).

**Data Availability Statement:** The data presented in this study are available on request from the corresponding author.

**Acknowledgments:** The authors are grateful to Taki Chemical Co., Ltd. for kindly donating PLGA-PEG-PLGA.

**Conflicts of Interest:** The authors declare no conflicts of interest.

## References

1. Zhou, X.; Chen, Y.; Cui, L.; Shi, Y.; Guo, C. Advances in the pathogenesis of psoriasis: From keratinocyte perspective. *Cell Death Dis.* **2022**, *13*, 81. [[CrossRef](#)] [[PubMed](#)]
2. Rendon, A.; Schäkel, K. Psoriasis pathogenesis and treatment. *Int. J. Mol. Sci.* **2019**, *20*, 1475. [[CrossRef](#)] [[PubMed](#)]
3. Ortonne, J.P.; Chimenti, S.; Luger, T.; Puig, L.; Reid, F.; Trüeb, R.M. Scalp psoriasis: European consensus on grading and treatment algorithm. *J. Eur. Acad. Dermatol. Venereol.* **2009**, *23*, 1435–1444. [[CrossRef](#)] [[PubMed](#)]
4. Nestle, F.O.; Kaplan, D.H.; Barker, J. Psoriasis. *N. Engl. J. Med.* **2009**, *361*, 496–509. [[CrossRef](#)] [[PubMed](#)]

5. Johnson-Huang, L.M.; Lowes, M.A.; Krueger, J.G. Putting together the psoriasis puzzle: An update on developing targeted therapies. *Dis. Model. Mech.* **2012**, *5*, 423–433. [[CrossRef](#)]
6. Chamian, F.; Lowes, M.A.; Lin, S.-L.; Lee, E.; Kikuchi, T.; Gilleaudeau, P.; Sullivan-Whalen, M.; Cardinale, I.; Khatcherian, A.; Novitskaya, I.; et al. Alefacept reduces infiltrating T cells, activated dendritic cells, and inflammatory genes in psoriasis vulgaris. *Proc. Natl. Acad. Sci. USA* **2005**, *102*, 2075–2080. [[CrossRef](#)] [[PubMed](#)]
7. Lowes, M.A.; Chamian, F.; Abello, M.V.; Fuentes-Duculan, J.; Lin, S.-L.; Nussbaum, R.; Novitskaya, I.; Carbonaro, H.; Cardinale, I.; Kikuchi, T.; et al. Increase in TNF- $\alpha$  and inducible nitric oxide synthase-expressing dendritic cells in psoriasis and reduction with efalizumab (anti-CD11a). *Proc. Natl. Acad. Sci. USA* **2005**, *102*, 19057–19062. [[CrossRef](#)] [[PubMed](#)]
8. Li, B.; Huang, L.; Lv, P.; Li, X.; Liu, G.; Chen, Y.; Wang, Z.; Qian, X.; Shen, Y.; Li, Y.; et al. The role of Th17 cells in psoriasis. *Immunol. Res.* **2020**, *68*, 296–309. [[CrossRef](#)] [[PubMed](#)]
9. Dattola, A.; Silvestri, M.; Tamburi, F.; Amoroso, G.F.; Bennardo, L.; Nisticò, S.P. Emerging role of anti-IL23 in the treatment of psoriasis: When humanized is very promising. *Dermatol. Ther.* **2020**, *33*, e14504. [[CrossRef](#)]
10. Dastoli, S.; Passante, M.; Loconsole, F.; Mortato, E.; Balato, A.; Piccolo, V.; Guarneri, C.; Macca, L.; Provenzano, E.; Valenti, G.; et al. Long-term efficacy and safety of secukinumab in real life: A 240 weeks multicenter study from Southern Italy. *J. Dermatolog. Treat.* **2023**, *34*, 2200868. [[CrossRef](#)]
11. Takeuchi, I.; Kagawa, A.; Makino, K. Skin permeability and transdermal delivery route of 30-nm cyclosporin A-loaded nanoparticles using PLGA-PEG-PLGA triblock copolymer. *Colloids Surf. A* **2020**, *600*, 124866. [[CrossRef](#)]
12. Frušić-Zlotkin, M.; Soroka, Y.; Tivony, R.; Larush, L.; Verkhovskiy, L.; Brégégère, F.M.; Neuman, R.; Magdassi, S.; Milner, Y. Penetration and biological effects of topically applied cyclosporin A nanoparticles in a human skin organ culture inflammatory model. *Exp. Dermatol.* **2012**, *21*, 938–943. [[CrossRef](#)] [[PubMed](#)]
13. Farkas, A.; Kemény, L.; Széll, M.; Dobozy, A.; Bata-Csörgo, Z. Ethanol and acetone stimulate the proliferation of HaCaT keratinocytes the possible role of alcohol in exacerbating psoriasis. *Arch. Dermatol. Res.* **2003**, *295*, 56–62. [[CrossRef](#)] [[PubMed](#)]
14. Tomoda, K.; Yabuki, N.; Terada, H.; Makino, K. Surfactant free preparation of PLGA nanoparticles: The combination of antisolvent diffusion with preferential solvation. *Colloids Surf. A* **2014**, *457*, 88–93. [[CrossRef](#)]
15. Takeuchi, I.; Kobayashi, S.; Hida, Y.; Makino, K. Estradiol-loaded PLGA nanoparticles for improving low bone mineral density of cancellous bone caused by osteoporosis: Application of enhanced charged nanoparticles with iontophoresis. *Colloids Surf. B* **2017**, *155*, 35–40. [[CrossRef](#)] [[PubMed](#)]
16. Takeuchi, I.; Suzuki, T.; Makino, K. Skin permeability and transdermal delivery route of 50-nm dexamethasone-loaded PLGA nanoparticles. *Colloids Surf. B* **2017**, *159*, 312–317. [[CrossRef](#)] [[PubMed](#)]
17. Xu, H.; Paxton, J.W.; Wu, Z. Enhanced pH-responsiveness, cellular trafficking, cytotoxicity and long-circulation of PEGylated liposomes with post-insertion technique using gemcitabine as a model drug. *Pharm. Res.* **2015**, *32*, 2428–2438. [[CrossRef](#)]
18. Huang, X.; Xu, M.Q.; Zhang, W.; Ma, S.; Guo, W.; Wang, Y.; Zhang, Y.; Gou, T.; Chen, Y.; Liang, X.J.; et al. ICAM-1-targeted liposomes loaded with liver X receptor agonists suppress PDGF-induced proliferation of vascular smooth muscle cells. *Nanoscale Res. Lett.* **2017**, *12*, 322. [[CrossRef](#)] [[PubMed](#)]
19. Barbieri, S.; Sonvico, F.; Como, C.; Colombo, G.; Zani, G.; Buttini, F.; Bettini, R.; Rossi, A.; Colombo, P. Lecithin/chitosan controlled release nanopreparations of tamoxifen citrate: Loading, enzyme-trigger release and cell uptake. *J. Control. Release* **2013**, *167*, 276–283. [[CrossRef](#)]
20. Takeuchi, I.; Ariyama, M.; Makino, K. Chitosan coating effect on cellular uptake of PLGA nanoparticles for boron neutron capture therapy. *J. Oleo Sci.* **2019**, *68*, 361–368. [[CrossRef](#)]
21. Hibino, M.; Sugiura, K.; Muro, Y.; Shimoyama, Y.; Tomita, Y. Cyclosporin A induces the unfolded protein response in keratinocytes. *Arch. Dermatol. Res.* **2011**, *303*, 481–489. [[CrossRef](#)] [[PubMed](#)]
22. Griffiths, C.E.; Katsambas, A.; Dijkmans, B.A.; Finlay, A.Y.; Ho, V.C.; Johnston, A.; Luger, T.A.; Mrowietz, U.; Thestrup-Pedersen, K. Update on the use of cyclosporin in immune-mediated dermatoses. *Br. J. Dermatol.* **2006**, *155* (Suppl. S2), 1–16. [[CrossRef](#)] [[PubMed](#)]
23. Kumar, R.; Philip, A. Modified transdermal technologies: Breaking the barriers of drug permeation via the skin. *Trop. J. Pharm. Res.* **2007**, *6*, 633–644. [[CrossRef](#)]
24. Godavarthy, S.S.; Yerramsetty, K.M.; Rachakonda, V.K.; Neely, B.J.; Madihally, S.V.; Robinson, R.L., Jr.; Gasem, K.A.M. Design of improved permeation enhancers for transdermal drug delivery. *J. Pharm. Sci.* **2009**, *98*, 4085–4099. [[CrossRef](#)]
25. van der Fits, L.; Mourits, S.; Voerman, J.S.A.; Kant, M.; Boon, L.; Laman, J.D.; Comelissen, F.; Mus, A.-M.; Florencia, E.; Prens, E.P.; et al. Imiquimod-induced psoriasis-like skin inflammation in mice is mediated via the IL-23/IL-17 axis. *J. Immunol.* **2009**, *182*, 5836–5845. [[CrossRef](#)] [[PubMed](#)]
26. Arora, R.; Katiyar, S.S.; Kushwah, V.; Jain, S. Solid lipid nanoparticles and nanostructured lipid carrier-based nanotherapeutics in treatment of psoriasis: A comparative study. *Expert Opin. Drug Deliv.* **2017**, *14*, 165–177. [[CrossRef](#)]
27. Kim, C.-H.; Kim, J.-Y.; Lee, A.-Y. Therapeutic and immunomodulatory effects of glucosamine in combination with low-dose cyclosporine A in a murine model of imiquimod-induced psoriasis. *Eur. J. Pharmacol.* **2015**, *756*, 43–51. [[CrossRef](#)]
28. Schindelin, J.; Arganda-Carreras, I.; Frise, E.; Kaynig, V.; Longair, M.; Pietzsch, T.; Preibisch, S.; Rueden, C.; Saalfeld, S.; Schmid, B.; et al. Fiji: An open-source platform for biological-image analysis. *Nat. Methods* **2012**, *9*, 676–682. [[CrossRef](#)]
29. Panonnummal, R.; Sabitha, M. Anti-psoriatic and toxicity evaluation of methotrexate chitin nanogel in imiquimod induced mice model. *Int. J. Biol. Macromol.* **2018**, *110*, 245–258. [[CrossRef](#)]

30. Kjær, T.N.; Thorsen, K.; Jessen, N.; Stenderup, K.; Pedersen, S.B. Resveratrol ameliorates imiquimod-induced psoriasis like skin inflammation in mice. *PLoS ONE* **2015**, *10*, e0126599. [[CrossRef](#)]
31. Jain, A.; Doppalapudi, S.; Domb, A.J.; Khan, W. Tacrolimus and curcumin co-loaded liposphere gel: Synergistic combination towards management of psoriasis. *J. Control. Release* **2016**, *243*, 132–145. [[CrossRef](#)] [[PubMed](#)]
32. de Porto, A.P.N.A.; Lammers, A.J.J.; Bennink, R.J.; ten Berge, I.J.M.; Speelman, P.; Hoekstra, J.B.L. Assessment of splenic function. *Eur. J. Clin. Microbiol. Infect. Dis.* **2010**, *29*, 1465–1473. [[CrossRef](#)]
33. Hatakeyama, H.; Akira, H.; Harashima, H. The polyethyleneglycol dilemma: Advantage and disadvantage of PEGylation of liposomes for systemic genes and nucleic acids delivery to tumors. *Biol. Pharm. Bull.* **2013**, *36*, 892–899. [[CrossRef](#)] [[PubMed](#)]
34. We, X.; Din, S.; Cai, H.; Wang, J.; Wen, L.; Yang, F.; Chen, G. Nanomedicine strategy for optimizing delivery to outer hair cells by surface-modified poly(lactic/glycolic acid) nanoparticles with hydrophilic molecules. *Int. J. Nanomed.* **2016**, *11*, 5959–5969. [[CrossRef](#)]
35. Halprin, K.M. Epidermal “turnover time”—A re-examination. *Br. J. Dermatol.* **1972**, *86*, 14–19. [[CrossRef](#)]
36. Takahashi, H.; Tsuji, H.; Minami-Hori, M.; Miyachi, Y.; Iizuka, H. Defective barrier function accompanied by structural changes of psoriatic stratum corneum. *J. Dermatol.* **2014**, *41*, 144–148. [[CrossRef](#)] [[PubMed](#)]
37. Sun, L.; Liu, Z.; Lin, Z.; Gun, D.; Tong, H.H.; Yan, R.; Wang, R.; Zheng, Y. Comparison of normal versus imiquimod-induced psoriatic skin in mice or penetration of drugs and nanoparticles. *Int. J. Nanomed.* **2018**, *13*, 5625–5635. [[CrossRef](#)]
38. Ma, H.-L.; Liang, S.; Li, J.; Napierata, L.; Brown, T.; Benoit, S.; Senices, M.; Gill, D.; Dunussi-Joannopoulos, K.; Collins, M.; et al. YIL-22 is required for Th17 cell-mediated pathology in a mouse model of psoriasis-like skin inflammation. *J. Clin. Invest.* **2008**, *118*, 597–607. [[CrossRef](#)]
39. Lynde, C.W.; Poulin, Y.; Vender, R.; Bourcier, M.; Khalil, S. Interleukin 17A: Toward a new understanding of psoriasis pathogenesis. *J. Am. Acad. Dermatol.* **2014**, *71*, 141–150. [[CrossRef](#)]
40. Van Belle, A.B.; de Heusch, M.; Lemaire, M.M.; Hendrickx, E.; Warnier, G.; Dunussi-Joannopoulos, K.; Fouser, L.A.; Renaud, J.-C.; Dumoutier, L. IL-22 is required for imiquimod-induced psoriasiform skin inflammation in mice. *J. Immunol.* **2012**, *188*, 462–469. [[CrossRef](#)]
41. Zaba, L.C.; Cardinale, I.; Gilleaudeau, P.; Sullivan-Whalen, M.; Suárez-Fariñas, M.; Fuentes-Duculan, J.; Novitskaya, I.; Khatcherian, A.; Bluth, M.J.; Lowes, M.A.; et al. Amelioration of epidermal hyperplasia by TNF inhibition is associated with reduced Th17 responses. *J. Exp. Med.* **2007**, *204*, 3183–3194. [[CrossRef](#)] [[PubMed](#)]
42. Yamamoto, S.; Jiang, H.; Kato, R. Stimulation of hair growth by topical application of FK506, a potent immunosuppressive agent. *J. Investig. Dermatol.* **1994**, *102*, 160–164. [[CrossRef](#)] [[PubMed](#)]
43. Hawkshaw, N.J.; Hardman, J.A.; Haslam, I.S.; Shahmalak, A.; Gilhar, A.; Lim, X.; Paus, R. Identifying novel strategies for treating human hair loss disorders: Cyclosporine A suppresses the Wnt inhibitor, SFRP1, in the dermal papilla of human scalp hair follicles. *PLoS Biol.* **2018**, *16*, e2003705. [[CrossRef](#)]

**Disclaimer/Publisher’s Note:** The statements, opinions and data contained in all publications are solely those of the individual author(s) and contributor(s) and not of MDPI and/or the editor(s). MDPI and/or the editor(s) disclaim responsibility for any injury to people or property resulting from any ideas, methods, instructions or products referred to in the content.